

Supporting Information

Bio-Based Macromolecular Polythiourethane Plasticizers Enable Sustainable and Migration-Resistant Flexible Films for Intelligent Packaging

Hong-Long Zheng, Wen-Tao Wang, Ting Liu, Ke Ma, En Zheng, Wen-Wu Zhang, Ke-Zheng Chen, Sheng-Lin Qiao**

Lab of Functional and Biomedical Nanomaterials, College of Materials Science and Engineering, Qingdao University of Science and Technology (QUST), Qingdao, 266042, P. R. China.

Corresponding authors: S.-L. Qiao (qiaosl@qust.edu.cn); K.-Z. Chen (kchen@qust.edu.cn).

KEYWORDS: macromolecular plasticizer, lipoic acid, polythiourethane, packaging, material recycling

Materials

Poly(ϵ -caprolactone) diol (PCL, $M_n=2000 \text{ g}\cdot\text{mol}^{-1}$), isophorone diisocyanate (IPDI), α -lipoic acid (LA), quercetin (QR, 97%), and polyvinyl chloride (PVC, commercial grade, Guangyuan Plastics) were used as received. Stannous octoate ($\text{Sn}(\text{Oct})_2$), N,N-dimethylformamide (DMF), tetrahydrofuran (THF), methanol, and deionized water were of analytical grade and used without further purification unless otherwise specified.

Synthesis of LPU

The lipoic acid-based polythiourethane (LPU) was synthesized using PCL diols as the soft segment. The molar ratio of $[\text{NCO}]$ (from IPDI) to $[\text{OH}]$ (from PCL) was set to 1.00 ($R=1.00$). The molar ratio of each component (PCL, IPDI, LA) is 1:3.5:2.5 in the reaction system. PCL diols were first introduced into a Schlenk system, heated in an oil bath at $120 \text{ }^\circ\text{C}$ under vacuum for 3h to remove moisture, and then cooled to approximately $65 \text{ }^\circ\text{C}$. A measured amount of IPDI and a few drops of stannous octoate catalyst (≈ 4 drops) were added via syringe under a nitrogen atmosphere, and the reaction mixture was stirred at $85 \text{ }^\circ\text{C}$ for 2h to obtain a viscous prepolymer. After three cycles of vacuum-nitrogen purging, the system was maintained under nitrogen protection. Subsequently, a predetermined amount of LA and 0.5 wt% $\text{Sn}(\text{Oct})_2$ were added rapidly under vigorous stirring, and the chain-extension reaction was carried out at $90 \text{ }^\circ\text{C}$ for 30 min. The resulting viscous product was transferred into an oven and cured overnight at $80 \text{ }^\circ\text{C}$ to yield transparent LPU.

Preparation of LPVC and DPVC Films

LPU and commercial DIOP were used as plasticizers to prepare LPVC and DPVC films, respectively. The mass ratios of plasticizer to PVC were set as $x=0, 0.1, 0.2, 0.3,$ and 0.4 . Predetermined amounts of LPU (or DIOP) and PVC were dissolved in anhydrous DMF and magnetically stirred for 12h to form 30wt% homogeneous solutions. The resulting mixtures were cast into glass Petri dishes and dried at $60 \text{ }^\circ\text{C}$ to remove solvent, producing uniform plasticized films. The obtained LPVC and DPVC samples were cut into dumbbell-and strip-shaped specimens for subsequent mechanical and thermal tests.

Reusability of LPVC

Used LPVC films (e.g., after mechanical testing or practical use) were collected and weighed into a single-neck flask. Anhydrous tetrahydrofuran (THF) was then added, and the mixture was magnetically stirred at room temperature (25 °C, 300 rpm) until the LPVC film was completely dissolved, yielding a homogeneous transparent viscous solution without visible solid particles or flocculent aggregates. The resulting LPVC/THF solution was then slowly poured into a clean glass Petri dish and spread uniformly by solution casting. Solvent removal was performed in two steps: first, drying at 40 °C for 6 h in a forced-air oven to gradually evaporate most of the THF and avoid rapid surface skinning, bubbles, or cracks; second, vacuum drying at 60 °C for 12 h to remove residual THF, affording a regenerated LPVC film with thickness, transparency, and flexibility comparable to those of the original sample. All solvent-handling operations were performed in a fume hood.

Characterization

FTIR and Raman Spectroscopy: Fourier transform infrared (FTIR) spectra were recorded on a Nicolet IS10 spectrometer in the range of 4000-400 cm^{-1} with a resolution of 4 cm^{-1} to identify characteristic functional groups. Raman spectra were also collected to complement molecular vibration analysis.

X-ray Diffraction (XRD): Crystalline structures were analyzed using a Rigaku D/MAX-2500PC diffractometer with Cu $K\alpha$ radiation ($\lambda=1.5406 \text{ \AA}$) operated at 18 kW. Data were collected at a scan rate of 5° min^{-1} over a 2θ range of 5° -60°.

UV-Vis Transmittance: Transmittance characterization of PVC and LPVCx and DPVCx with varying LPU and DIOP additions was performed using a UV2600i UV-Vis spectrophotometer. The measurement range was 200–800 nm, with the test speed set to medium.

X-ray Photoelectron Spectroscopy (XPS): Surface elemental compositions and chemical states were determined using a Thermo Fisher Scientific XPS system equipped with a five-axis manipulator, providing an energy resolution better than 0.43 eV. Characterization of LA and its products LPU and LPVC was performed using ESCALAB Xi+ photoelectron spectroscopy. The experiment characterized structural and valence state changes for four elements: S, Cl, O, and C.

Scanning Electron Microscopy (SEM): Surface morphologies of LPVC and DPVC films were examined using a JEOL JSM-6700F field-emission scanning electron microscope operated at 8 kV and a beam current of 10 μ A. Microstructural changes were correlated with the incorporation of quercetin.

Thermogravimetric Analysis (TGA): Thermal stability was assessed on a NETZSCH TG209F1-Libra analyzer under a nitrogen atmosphere. Samples were heated from room temperature to the decomposition point at a rate of 10 $^{\circ}$ C min^{-1} .

Mechanical Testing: Uniaxial tensile tests were performed at room temperature using a universal testing machine equipped with a 100N load cell. Dumbbell-shaped specimens were stretched at a crosshead speed of 50 mm min^{-1} . Fracture toughness was evaluated using notched rectangular specimens (0.5 mm \times 20 mm \times 10 mm) with a notch length of approximately 4 mm (\sim 1/5 of the width).

Thermogravimetric Analysis (TGA) Characterization: Using the TG/DTA 8122 instrument, PVC, LPVC, and DPVC samples in crucibles were heated from room temperature to 650 $^{\circ}$ C at a heating rate of 10 $^{\circ}$ C min^{-1} under a nitrogen atmosphere to investigate their TG curves.

Dynamic Mechanical Analysis (DMA): DMA measurements were carried out on a PerkinElmer DMA 8000 in tensile mode using rectangular samples (30 mm \times 4 mm \times 0.7 mm). The temperature was ramped from 30 $^{\circ}$ C to 80 $^{\circ}$ C at 3 $^{\circ}$ C min^{-1} with a 10 mm clamp spacing. An oscillation strain of 0.1% was applied to ensure linear viscoelastic conditions.

CCK-8 Cell Viability Assay: Prepare LPVC immersion solutions of 0, 50, 100, 150, and 200 μ L using 10 \times PBS buffer as the solvent, with a concentration of 50 mg/mL. Add 1000, 950, 900, 850, and 800 μ L of DMEM medium sequentially to the above volumes of extraction solution to prepare extracts with concentrations of 0, 2.5, 5, 7.5, and 10 mg/mL, respectively. L929 cells were seeded at a density of 5×10^3 cells per well in a 96-well plate, with 100 μ L of cell suspension added to each well. The cells were cultured in DMEM medium supplemented with 10% fetal bovine serum at 37 $^{\circ}$ C and 5% CO_2 for 12 hours. After incubation, cells were washed three times with PBS. Each well received 10 μ L CCK-8 solution and was incubated for an additional 4 hours at 37 $^{\circ}$ C under 5% CO_2 . The absorbance of each well was measured at 450 nm using a microplate reader (blank control: medium without LPVC).

Supplementary Figures

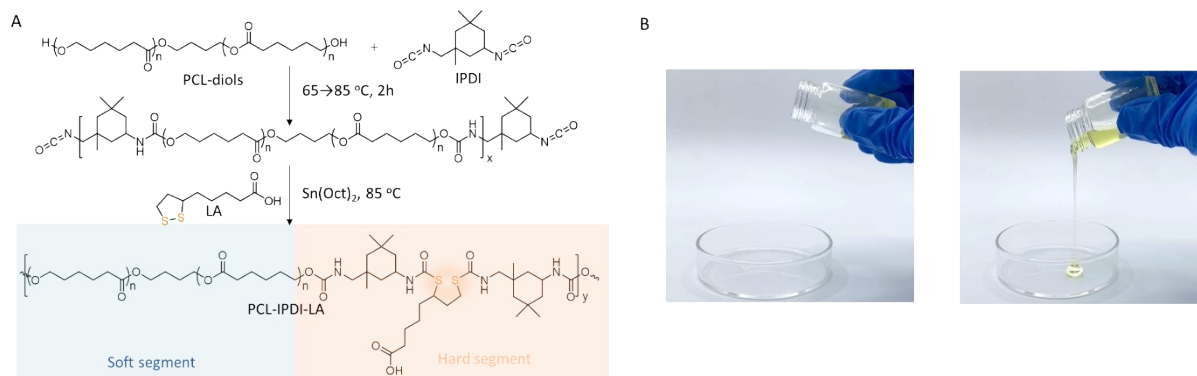


Figure S1. (A) The synthesis process of LPU. (B) Photographic illustrating fluid character of the synthesized LPU plasticizer.

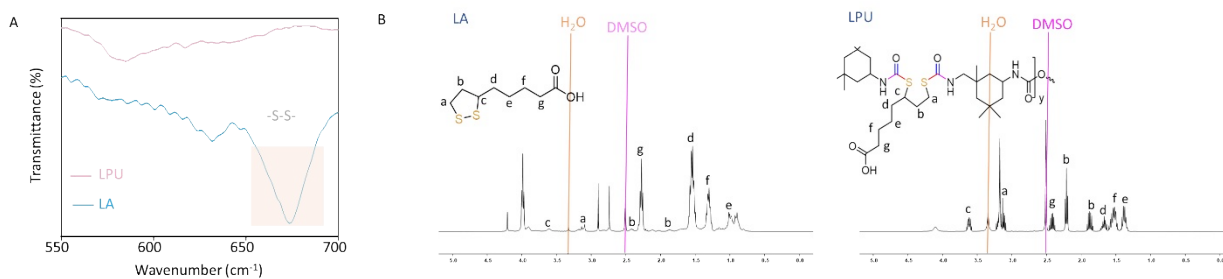


Figure S2. (A) FTIR spectra of LA and LPU in the wavenumber range 550-700 cm^{-1} . (B) ^1H NMR spectra of LA and LPU.

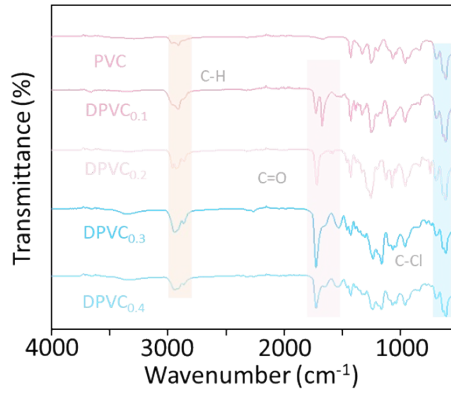


Figure S3. FTIR spectra of neat PVC film and DPVC_{0.1}, DPVC_{0.2}, DPVC_{0.3}, and DPVC_{0.4} films plasticized with commercial-grade DIOP.

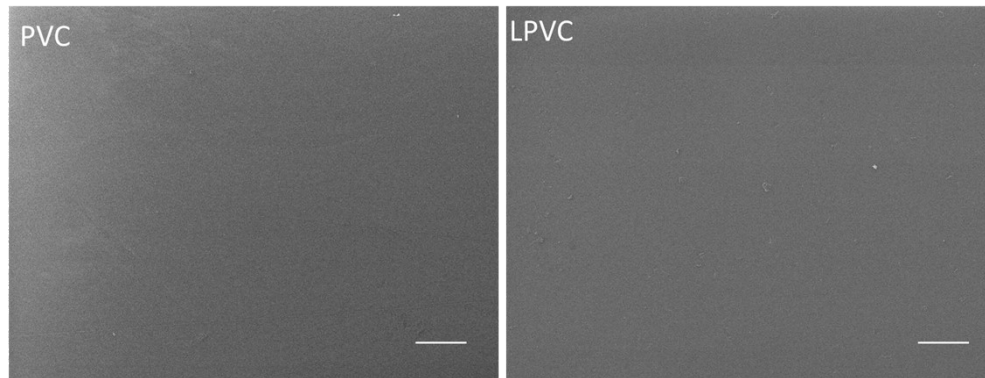


Figure S4. SEM images of the surfaces of neat PVC and PVC plasticized with LPU, 100 μm.

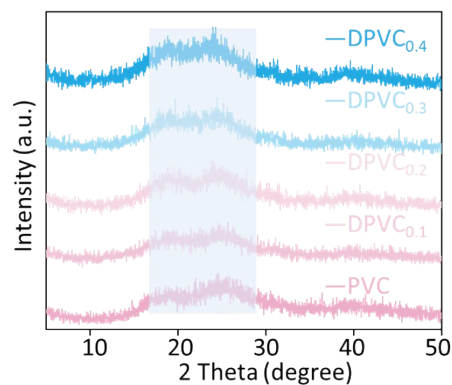


Figure S5. XRD patterns of neat PVC film and DPVC_{0.1}, DPVC_{0.2}, DPVC_{0.3}, and DPVC_{0.4} films plasticized with commercial-grade DIOP.

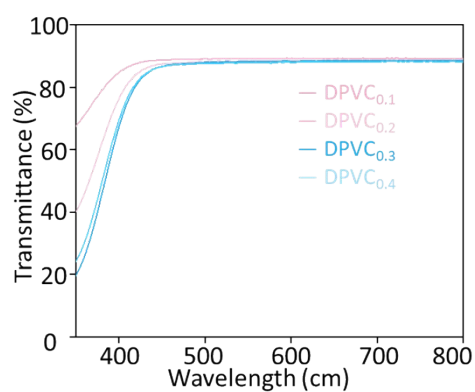


Figure S6. UV-vis transmittance spectra of DPVC_{0.1}, DPVC_{0.2}, DPVC_{0.3}, and DPVC_{0.4} films plasticized with commercial-grade DIOP.



Figure S7. Photographs illustrating the optical transmittance of neat PVC and PVC films plasticized with different amounts of DIOP and LPU.

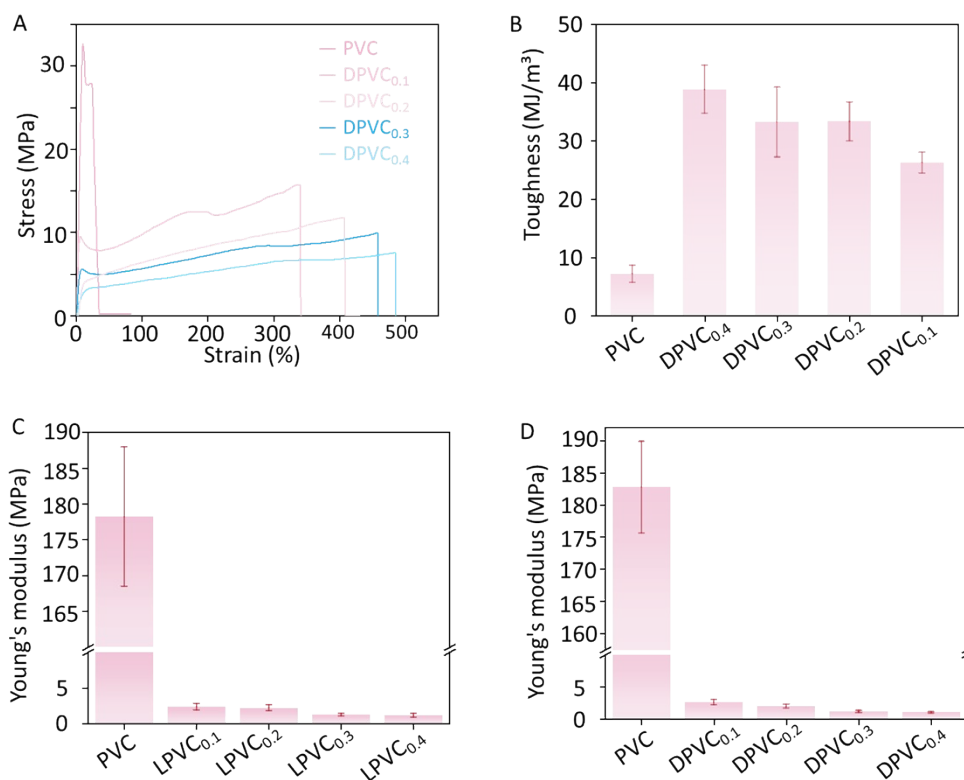


Figure S8. (A) Stress-strain curves and (B) comparison of toughness for neat PVC and DPVC_{0.1}, DPVC_{0.2}, DPVC_{0.3}, and DPVC_{0.4} films plasticized with commercial-grade DIOP. (C) Comparison of the Young's modulus of pristine PVC and LPVC films. (D) Comparison of the Young's modulus of PVC and DPVC films.

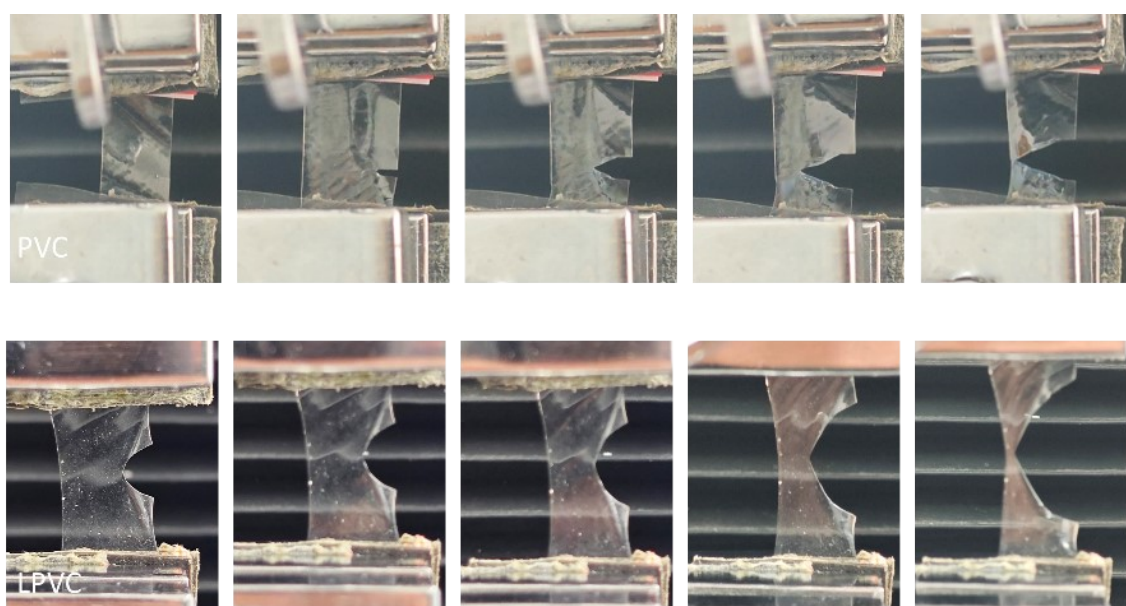


Figure S9. Photographic image of the evolution of notch fracture in neat PVC and LPU-plasticized LPVC.

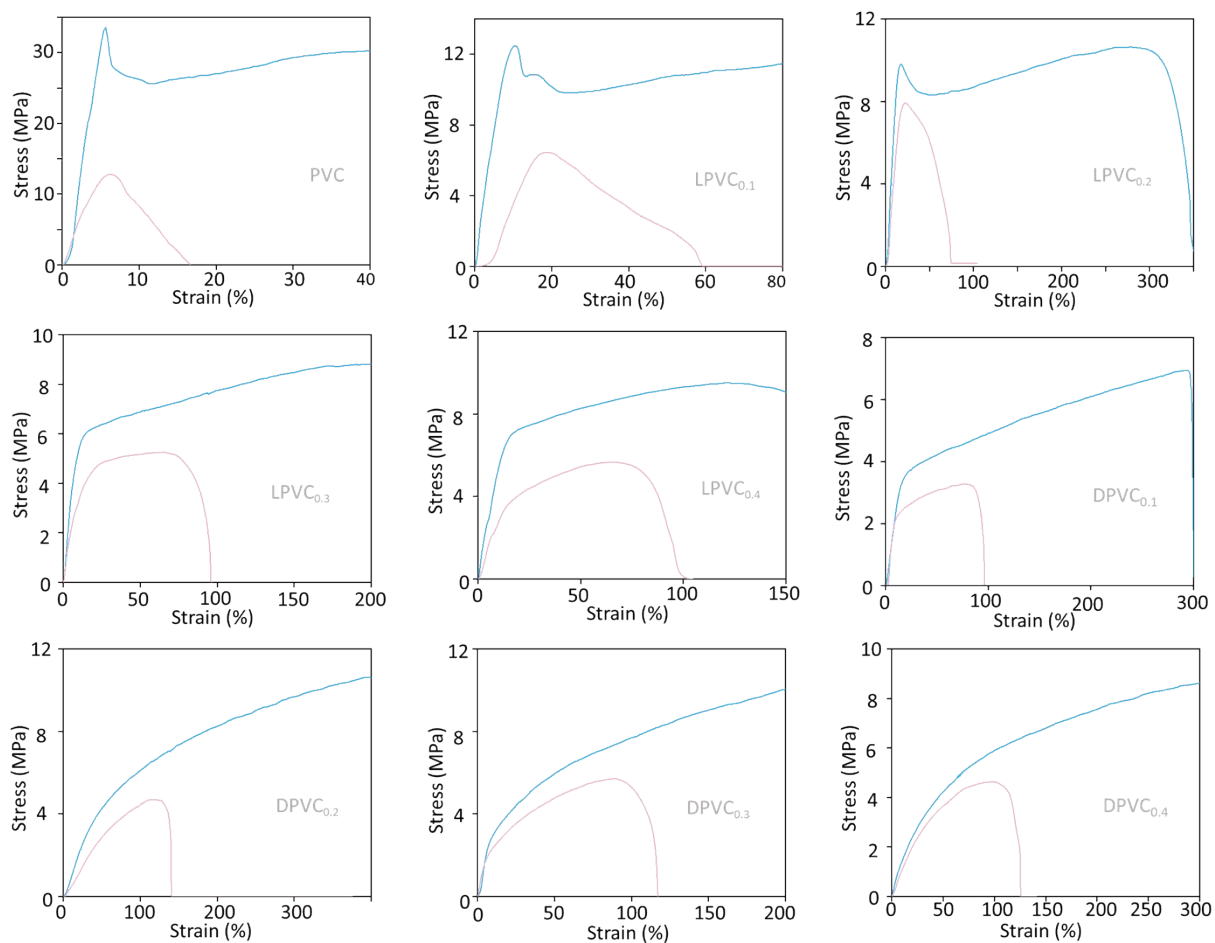


Figure S10. Stress-strain curves of neat PVC, LPVC, and DPVC films under notched and unnotched conditions.

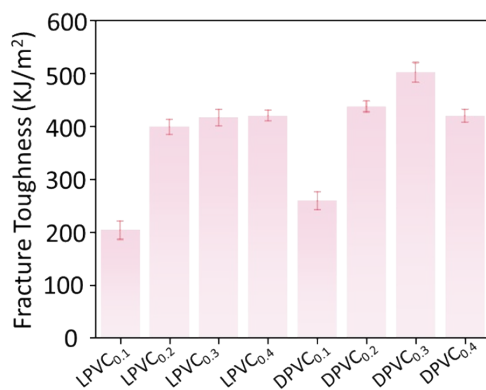


Figure S11. Fracture toughness of neat PVC, LPVC, and DPVC under notched fracture conditions.

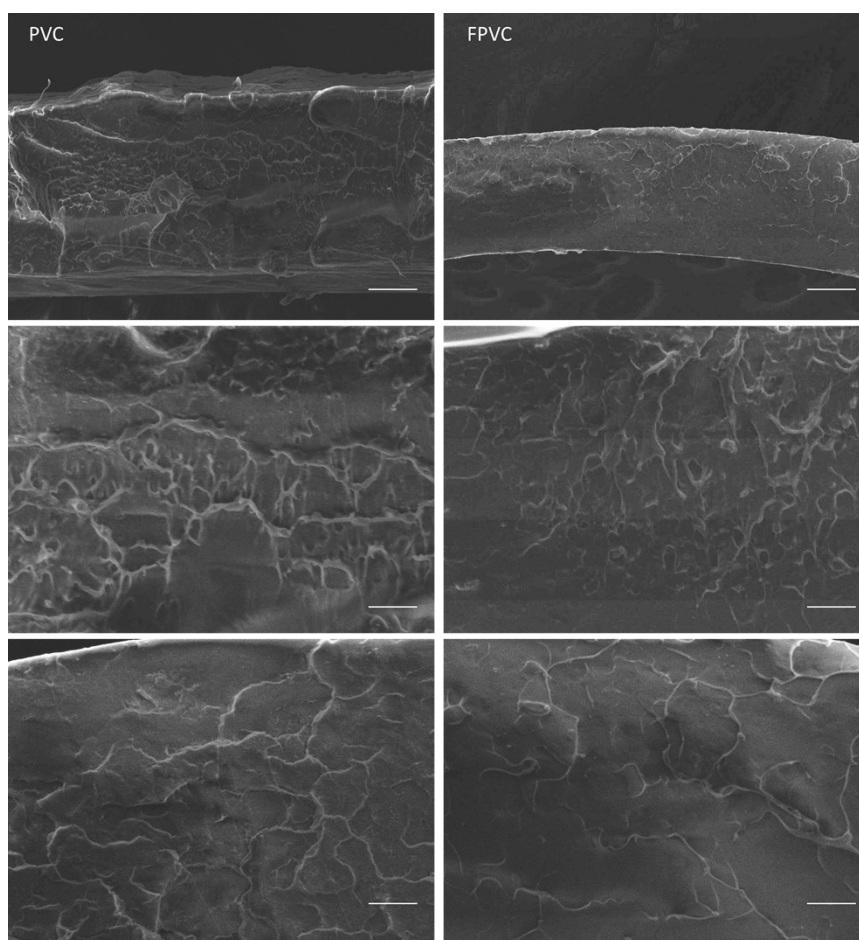


Figure S12. SEM micrographs of the notched fracture surfaces of neat PVC and LPVC films. Scale bar, 100 μm .

Table S1. XPS data for LPVC, PVC, and LPU regarding Cl and S elements before and after feeding.

Sample Type	Cl Atomic Percentage	S Atomic Percentage	Note
LPVC	4.31%	1.06%	Hybrid product containing two characteristic elements
PVC	15.29%	0%	Contains only Cl, no S
LPU	0%	5.75%	Contains only S, no Cl

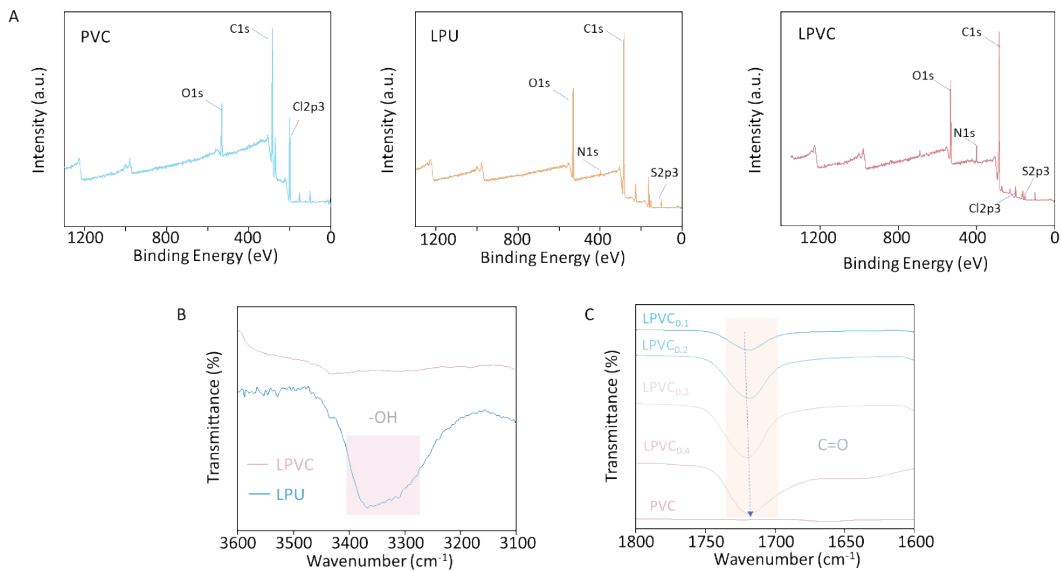


Figure S13. (A) XPS spectrum of PVC, LPU and LPVC (LPU: PVC=4:6). (B) FTIR spectra of LPVC and LPU in the wavenumber range 3100-3600 cm^{-1} . (C) FTIR spectra of neat PVC and LPVC_{0.1}, LPVC_{0.2}, LPVC_{0.3}, and LPVC_{0.4} in the wavenumber range 1600-1800 cm^{-1} .

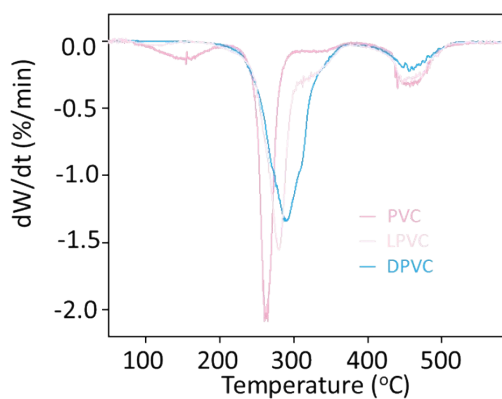


Figure S14. DTG curves of neat PVC and LPVC.

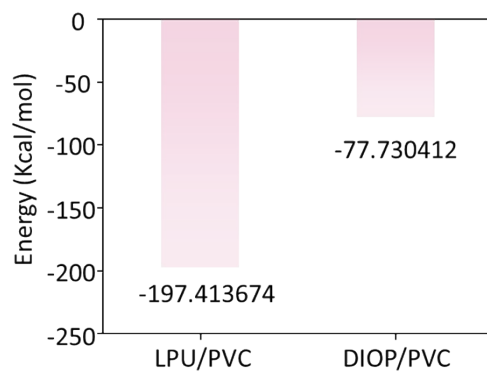


Figure S15. Binding energies of LPU, DIOP, and PVC.

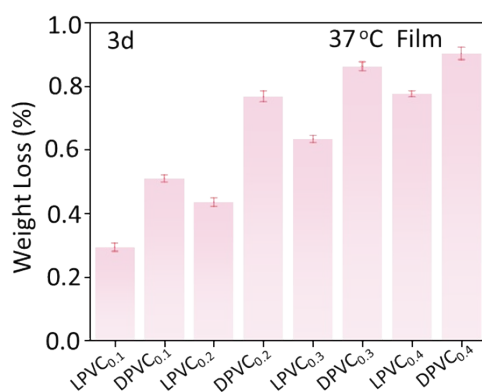


Figure S16. Plasticizer migration rates of LPVC_{0.1}, LPVC_{0.2}, LPVC_{0.3}, LPVC_{0.4}, DPVC_{0.1}, DPVC_{0.2}, DPVC_{0.3}, and DPVC_{0.4} films prepared via a coating method.

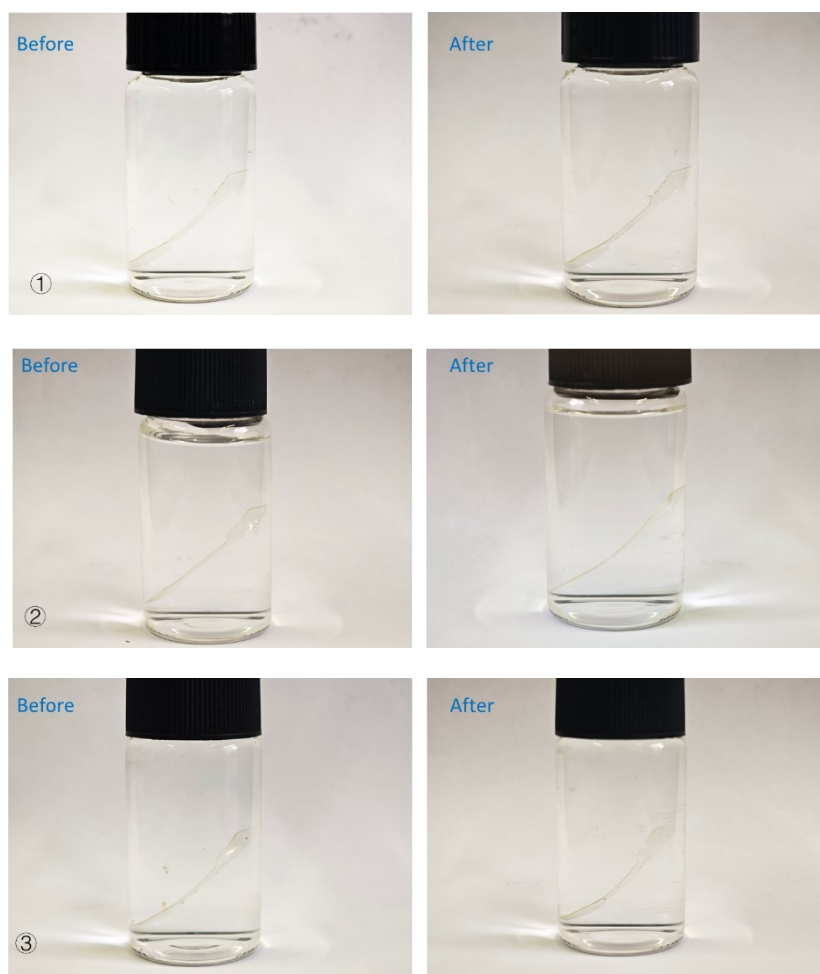


Figure S17. Solubility and swelling test of LPVC film in water.

Table S2. Mass change and water solubility of three sets of dumbbell-shaped LPVC samples after water immersion.

Sample	M_{before} (g)	M_{after} (g)	QM (%)
1	0.0387	0.0385	0.519
2	0.0335	0.0332	0.904
3	0.0344	0.0341	0.880

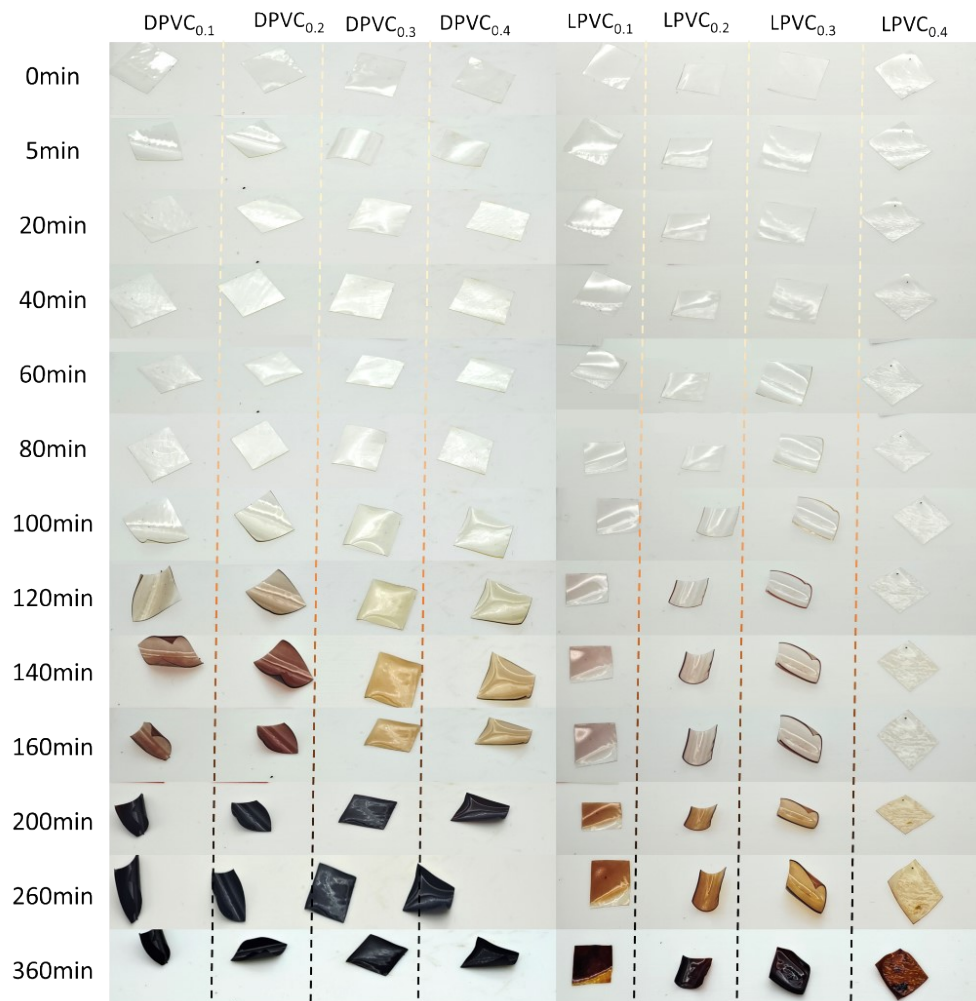


Figure S18. Aging behavior of LPVC_{0.1}, LPVC_{0.2}, LPVC_{0.3}, LPVC_{0.4}, DPVC_{0.1}, DPVC_{0.2}, DPVC_{0.3}, and DPVC_{0.4} films evaluated at different time intervals.



Figure S19. Anti-puncture test of LPVC films.

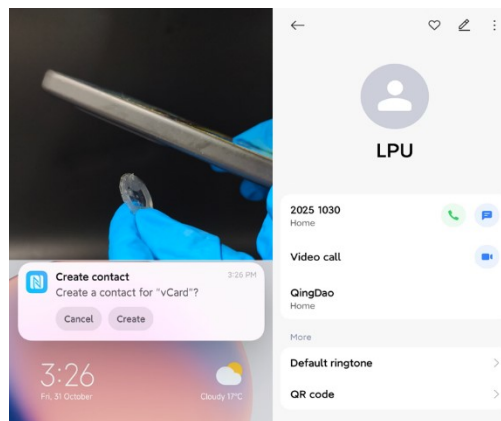


Figure S20. Long-term stability of the measured signal, which remains essentially unchanged over 6 months.